Transport and Communications Science Journal, Vol 75, Issue 1 (01/2024), 1159-1168

Transport and Communications Science Journal

COMPUTATION OF THE EFFECTIVE PERMEABILITY OF 2D DOUBLY POROUS MATERIALS WITH ELLIPTICAL SHAPED PORES BY USING BOUNDARY ELEMENT METHOD

Tran Anh Tuan, Tran Thi Bich Thao*

University of Transport and Communications, No 3 Cau Giay Street, Hanoi, Vietnam

ARTICLE INFO

TYPE: Research Article
Received: 09/11/2023
Revised: 21/12/2023
Accepted: 08/01/2024
Published online: 15/01/2024
https://doi.org/10.47869/tcsj.75.1.5

* *Corresponding author*
Email: tbthao.tran@utc.edu.vn

Abstract. In recent years, the prediction of the effective transport properties have received a great number of investigations. The present work is dedicated to determining the effective permeability of two-dimensional (2D) doubly porous materials made of an isotropic permeable solid matrix in which elliptical shaped pores of any size are embedded. At the interface between the fluid and the solid, the Beaver–Joseph–Saffman conditions are applied. To achieve this objective, the Boundary Element Method (BEM) is first elaborated in the simulation of velocity and pressure solution fields of two coupled Stokes and Darcy problems. Afterwards, with the help of this solution results, the effective permeablity of the doubly porous material under investigation can be determined. For the purpose of assessing the accuracy and convergence of the BEM solution, the results obtained for the velocity and pressure fields are compared with the ones provided by the finite element method (FEM). Finally, several numerical examples are carried out to analyze the fluid/solid interface influence, the effect of area fraction and geometrical properties of pores, such as the size and distribution of the pores within the matrix phase.

Keywords: BEM, effective permeability, double porosity, coupled Stokes-Darcy problem, fluid-filled inclusion.

1. INTRODUCTION

Most of natural and artificial materials such as soil, rock, concrete etc. can be naturally considered as doubly porous media. For example, in fractured concretes, the first level porosity consists of small-scale intergranular pores whereas the larger scale fractures and cavities lie so that to the second porosity level. In dealing with this kind of materials, the prediction of the effective transport properties have attracted a great number of investigations of the research community in recent years. In the present paper, we focus on the determination of the macroscopic permeability of doubly porous media containing saturated pores. Here, the domain under consideration is modeled by a host solid matrix in which nonconnected fluid-filled inclusions of elliptical shape are randomly distributed and orientated. In the host matrix, the flow is described by the Darcy equation while in the pores inclusions the fluid flow does not obey Darcy's law, rather, it is governed by Stokes equation. Thus, with the purpose to estimate the macroscopic permeability of doubly porous materials, we need to solve the coupling Stokes-Darcy flow problem in which the fluid-solid interface conditions are described by Beaver–Joseph–Saffman equations [1,2].

There are various approaches for determining the permeability of porous materials reported in the literature. This includes homogenization methods based on asymptotic expansion [3,4] or on volume average method applied to random microstructure [5]. When the microstructure of porous materials becomes complex, the classical numerical approach based on the finite element method [6-10] or fast Fourier transform [11-13] can be applied to compute the macroscopic permeability. In the present work, the flow and transport process through porous media under consideration is simulated by the Boundary Element Method (BEM). Note that in this numerical method, the velocity and pressure solution fields are presented in terms of integrals, involving the unknown tractions, velocities, pressures and fluxes over the external boundary and interfaces (also called boundary/interface values). These boundary values are then obtained by solving a system of linear equations, which results from matching the prescribed external boundary and fluid/solid interfaces conditions. It is well-known that singular integrals are a difficulty needed to overcome when using the BEM. In this work, these singular integrals are evaluated analytically.

The remaining sections of this paper are structured as follows. Section 2 is dedicated to specifying the setting of the problem under investigation. Precisely, the local governing equations, the description of the interface conditions, the macroscopic constitutive equations are given and then the coupled Darcy–Stokes problem of a fluid flowing through a porous medium is numerically solved by BEM. In Section 3, some examples are given to numerically illustrate the velocity and pressure solution fields within the computational domain and to show the dependence of the effective permeability on the interfacial parameter, on the geometrical properties and area fraction of pore inclusion. Finally, the work closes in Section 4 with a few concluding remarks.

2. PROBLEM SETTING

The doubly porous material under consideration is assumed to be formed of a solid matrix phase in which the fluid-filled pore inclusions of elliptical shape are scattered throughout. The domain occupied by a representative area element (RAE) of this material is denoted by Ω. More precisely, we designate by $\Omega^{(0)}$ and $\Omega^{(i)}(i = 1,2,\cdots,N)$ the subdomains of Ω occupied by the solid phase and the i-th pore (see Fig. 1). The interface between the solid

phase and the fluid-filled inclusion phase is symbolized by $\Gamma^{(i)}$. In addition, the fluid flow within the RAE is generated by a uniform prescribed pressure gradient at infinity $\hat{p}(\mathbf{x}) = -\mathbf{G}\cdot\mathbf{x}$, here $\mathbf{G} = (G\cos\theta + G\sin\theta)$ and θ stands for the angle between the pressure gradient vector $\mathbf{G}$ and the x-axis.

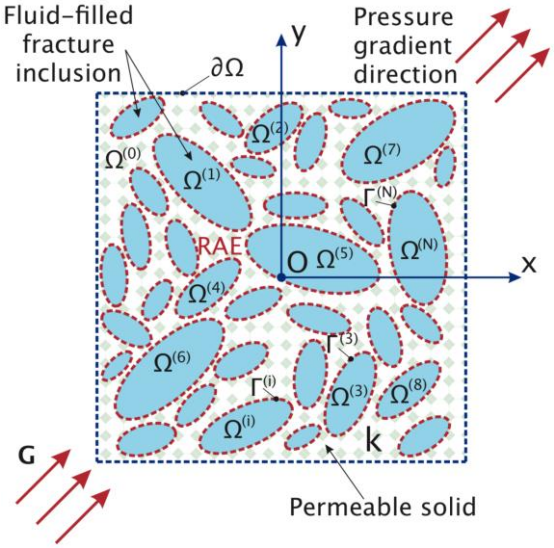

Figure 1. Representative Area Element of doubly porous media.

Now and hereafter, it is important to notice that all the local governing equations in this work will be expressed in the dimensionless forms by the help of choosing $L, \frac{GL^2}{\mu}, L^2, G$ and GL as the length, velocity, permeability, pressure gradient and pressure, respectively. Where L denote the dimension of RAE and μ designates the viscosity of the fluid. The fluid flow inside the pores is assumed to be incompressible, steady and governed by the following Stokes equations

$$\Delta\mathbf{u}^{(\mathrm{f})}(\mathbf{x})=\nabla p^{(\mathrm{f})}(\mathbf{x}), \qquad \nabla\cdot\mathbf{u}^{(\mathrm{f})}(\mathbf{x})=0, \qquad \mathbf{x}\in\Omega^{(i)}, \tag{1}$$

where $\mathbf{u}^{(\mathrm{f})}(\mathbf{x})$ và $p^{(\mathrm{f})}(\mathbf{x})$ are the velocity and pressure fields of the fluid in the pores $\Omega^{(i)}$.

The solid matrix subdomain of the doubly porous material under consideration is assumed to be homogeneous and isotropic. Thus, the fluid flow through the latter complies with the Darcy' law as follows

$$\mathbf{u}^{(\mathrm{s})}(\mathbf{x})=-k\nabla p^{(\mathrm{s})}(\mathbf{x}), \qquad \mathbf{x}\in\Omega^{(0)}, \tag{2}$$

where $\mathbf{u}^{(\mathrm{s})}(\mathbf{x})$ and $p^{(\mathrm{s})}(\mathbf{x})$ are, respectively, the fluid velocity and pressure fields within the solid subdomain and k denotes its permeability.

The interfacial conditions at the fluid/solid interface $\Gamma^{(i)}$ can be described by using the Beavers–Joseph–Saffman conditions [1, 2]

$$\mathbf{u}^{(\mathrm{f})}(\mathbf{x})\cdot\mathbf{n}(\mathbf{x})=\mathbf{u}^{(\mathrm{s})}(\mathbf{x})\cdot\mathbf{n}(\mathbf{x}), \qquad \mathbf{x}\in\Gamma^{(i)}, \tag{3}$$

$$[\mathbf{u}^{(\mathrm{f})}(\mathbf{x})-\mathbf{u}^{(\mathrm{s})}(\mathbf{x})]\cdot\mathbf{t}(\mathbf{x})=-\lambda\sqrt{k}\left[\boldsymbol{\sigma}^{(\mathrm{f})}(\mathbf{x})\cdot\mathbf{n}(\mathbf{x})\right]\cdot\mathbf{t}(\mathbf{x}), \qquad \mathbf{x}\in\Gamma^{(i)}, \tag{4}$$

$$p^{(\mathrm{f})}(\mathbf{x})-p^{(\mathrm{s})}(\mathbf{x})=\mu\,\mathbf{n}(\mathbf{x})\cdot\left[\nabla\mathbf{u}^{(\mathrm{f})}(\mathbf{x})+\nabla^{\mathrm{T}}\mathbf{u}^{(\mathrm{s})}(\mathbf{x})\right]\cdot\mathbf{n}(\mathbf{x}), \qquad \mathbf{x}\in\Gamma^{(i)}. \tag{5}$$

Above, $\mathbf{n}$ is the outward unit vector normal to $\Gamma^{(i)}$ while $\mathbf{t}$ stands for the unit tangential vector, $\boldsymbol{\sigma}^{(\mathrm{f})}$ denotes the Cauchy stress tensor in the Stokes subdomain and λ is slip coefficient.

The velocity and pressure solution fields of the coupled Darcy–Stokes problem will be determined by using an approach based on the BEM, sometimes called also the boundary integral method. These solution fields can be expressed as four following integral formulations

$$\epsilon(\boldsymbol{\xi})\mathbf{u}^{(\mathrm{f})} = -\int_{\Gamma^{(i)}} \boldsymbol{\tau}^{(\mathrm{f})}(\mathbf{x})\cdot\mathbf{S}(\mathbf{x},\boldsymbol{\xi})\,\mathrm{dl}(\mathbf{x}) - \int_{\Gamma^{(i)}} \mathbf{u}^{(\mathrm{f})}(\mathbf{x})\cdot\mathfrak{T}(\mathbf{x},\boldsymbol{\xi})\cdot\mathbf{n}(\mathbf{x})\,\mathrm{dl}(\mathbf{x}), \tag{6}$$

$$\epsilon(\boldsymbol{\xi})p^{(\mathrm{f})} = \int_{\Gamma^{(i)}} \boldsymbol{\tau}^{(\mathrm{f})}(\mathbf{x})\cdot\mathbf{f}(\mathbf{x},\boldsymbol{\xi})\,\mathrm{dl}(\mathbf{x}) + \int_{\Gamma^{(i)}} \mathbf{u}^{(\mathrm{f})}(\mathbf{x})\cdot\boldsymbol{\Theta}(\mathbf{x},\boldsymbol{\xi})\cdot\mathbf{n}(\mathbf{x})\,\mathrm{dl}(\mathbf{x}), \tag{7}$$

$$\mathrm{c}(\boldsymbol{\xi})p^{(\mathrm{s})} = -\int_{\partial\Omega\cup\Gamma^{(i)}} q^{(\mathrm{s})}(\mathbf{x})g(\mathbf{x},\boldsymbol{\xi})\,\mathrm{dl}(\mathbf{x}) + \int_{\partial\Omega\cup\Gamma^{(i)}} p^{(\mathrm{s})}(\mathbf{x})h(\mathbf{x},\boldsymbol{\xi})\,\mathrm{dl}(\mathbf{x}), \tag{8}$$

$$\mathrm{c}(\boldsymbol{\xi})\mathbf{u}^{(\mathrm{s})} = k\int_{\partial\Omega\cup\sum\Gamma^{(i)}} q^{(\mathrm{s})}(\mathbf{x})\nabla g(\mathbf{x},\boldsymbol{\xi})\,\mathrm{dl}(\mathbf{x}) - k\int_{\partial\Omega\cup\sum\Gamma^{(i)}} p^{(\mathrm{s})}(\mathbf{x})\nabla h(\mathbf{x},\boldsymbol{\xi})\,\mathrm{dl}(\mathbf{x}), \tag{9}$$

where ϵ and c are the constants dependent on the position of the source point $\boldsymbol{\xi}$ given by

$$\mathrm{c}(\boldsymbol{\xi})/\epsilon(\boldsymbol{\xi}) = \begin{cases} 1 \text{ for } \boldsymbol{\xi} \text{ inside } \Omega^{(0)}/\Omega^{(i)}, \\ \dfrac{1}{2} \text{ for } \boldsymbol{\xi} \text{ on the boundary } \partial\Omega \cup \Gamma^{(i)}/\Gamma^{(i)}, \\ 0 \text{ for } \boldsymbol{\xi} \text{ outside } \Omega^{(0)}/\Omega^{(i)}. \end{cases} \tag{10}$$

Above, $\boldsymbol{\tau}^{(\mathrm{f})}$, $\mathbf{u}^{(\mathrm{f})}$, $q^{(\mathrm{s})}$, $p^{(\mathrm{s})}$ are the unknown traction, velocity, flux and pressure at the field point $\mathbf{x}$ lying on the internal interface $\Gamma^{(i)}$ and external boundary $\partial\Omega$; $\mathbf{S}$, $\mathfrak{T}$, $\mathbf{f}$, $\boldsymbol{\Theta}$, g, h are the Stokeslet, the third-order stress Green's tensor, the pressure vector associated with the Stokeslet, the second-order pressure tensor associated with the stresslet, the fundamental solution for the pressure and flux, respectively. For more details about these Green's functions, the reader can refer to the books of Pozrikidis [14] and Katsikadelis [15].

At the macroscopic scale, the doubly porous material under investigation is assumed to be statistically homogeneous. Thus, its effective behavior is characterized by the following macroscopic Darcy's equation

$$\overline{\mathbf{U}} = -\mathbf{K}^{\mathrm{eff}}\overline{\nabla P} \tag{11}$$

with

$$\mathbf{K}^{\mathrm{eff}} = \begin{bmatrix} k^{\mathrm{eff}} & 0 \\ 0 & k^{\mathrm{eff}} \end{bmatrix}. \tag{12}$$

Where, $\mathbf{K}^{\mathrm{eff}}$ stands for the effective permeability tensor of the RAE; $\overline{\mathbf{U}}$, $\overline{\nabla P}$ denote the macroscopic velocity and pressure gradient, they are determined by

$$\overline{\mathbf{U}} = \frac{1}{S}\int_{\partial\Omega} [\mathbf{u}^{(s)}(\mathbf{x})\cdot\mathbf{v}(\mathbf{x})]\mathbf{x}d\mathbf{x} \tag{13}$$

and

$$\overline{\nabla P} = \frac{1}{S}\int_{\partial\Omega} p^{(s)}(\mathbf{x})\cdot\mathbf{v}(\mathbf{x})\, d\mathbf{x} \tag{14}$$

with $\partial\Omega$ is external boundary of Ω, $\mathbf{v}(\mathbf{x})$ designate the outward unit vector normal to $\partial\Omega$, while S denotes the area of RAE.

3. NUMERICAL EXAMPLES, COMPARISONS AND DISCUSSION

In this section, the methods elaborated in the previous sections are now applied to study several examples. We numerically calculate in the first example the velocity and pressure fields of porous materials containing nonconnected pore inclusions of elliptical shape randomly distributed (see Fig. 2). Notice that the fluid flow through the RAE by an applied pressure gradient of intensity $G = 1$ along the *x*-direction. In addition, the slip coefficient λ is set to be equal to 0 and the normalized permeability of the host matrix is chosen such as $k = 0.01$.

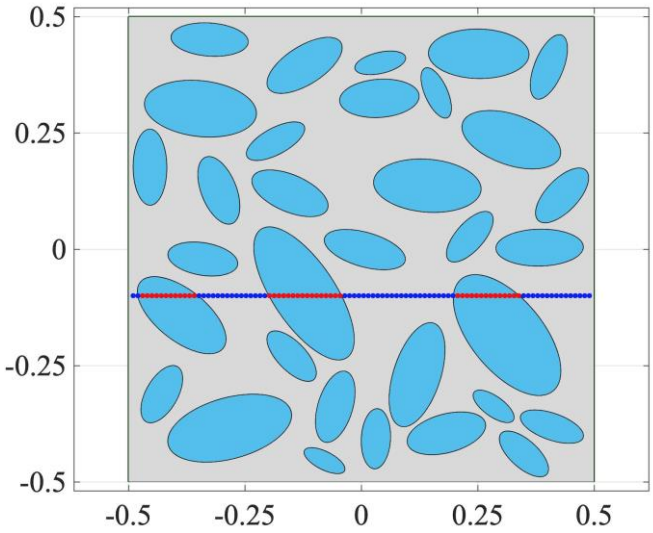

Figure 2. Position's line for the computations of velocity and pressure

We show, in Figs. 3 and 4, the variation of the normalized fluid velocity and pressure for points located on the line $y = -0{,}1$ (see Fig. 2). The values obtained by BEM for velocity and pressure then compared with the corresponding ones provided by FEM via Comsol Multiphysics software. With the help of Comsol Multiphysics, the computational domain was first discretized using 43914 triangular elements with 22149 mesh points as shown in Fig. 3. Plot of pressure solution field is shown in Fig. 4. A very good agreement between these results can be observed from Figs. 5 and 6.

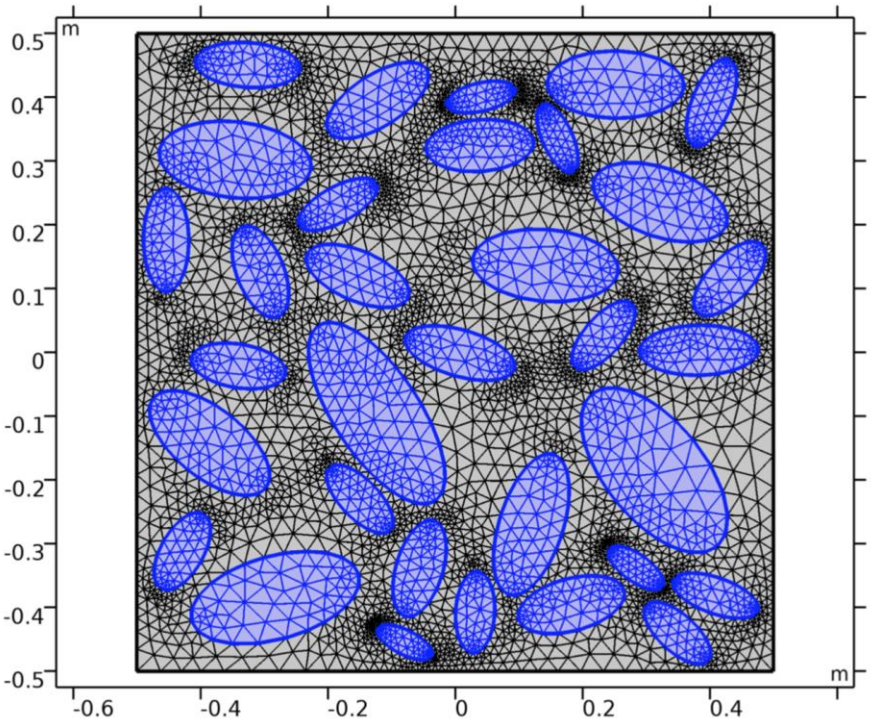

Figure 3. Discretization of computational domain.

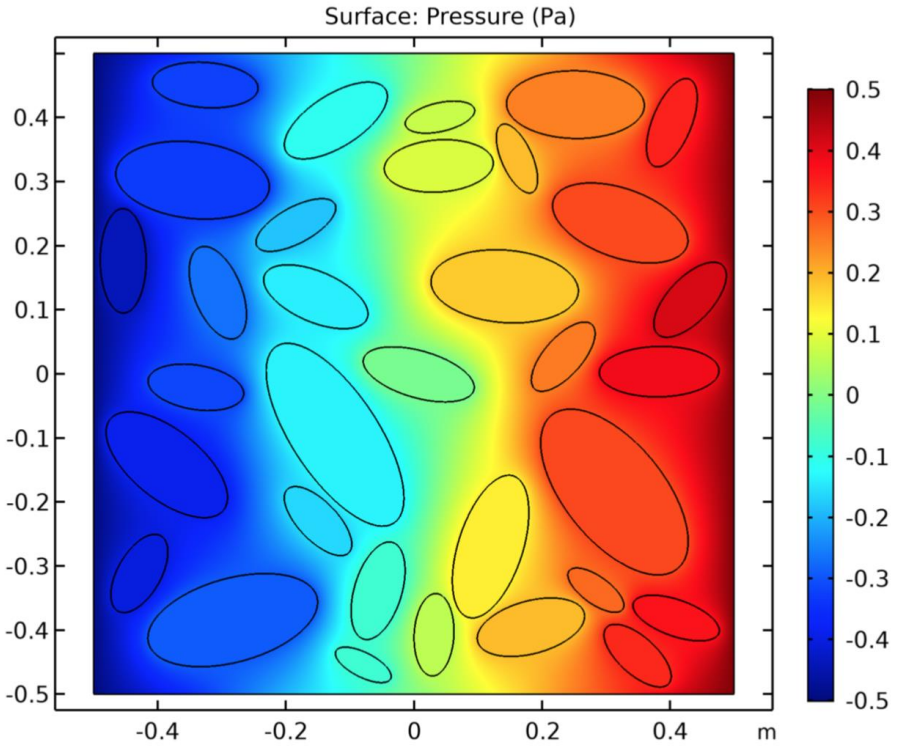

Figure 4. Pressure solution field.

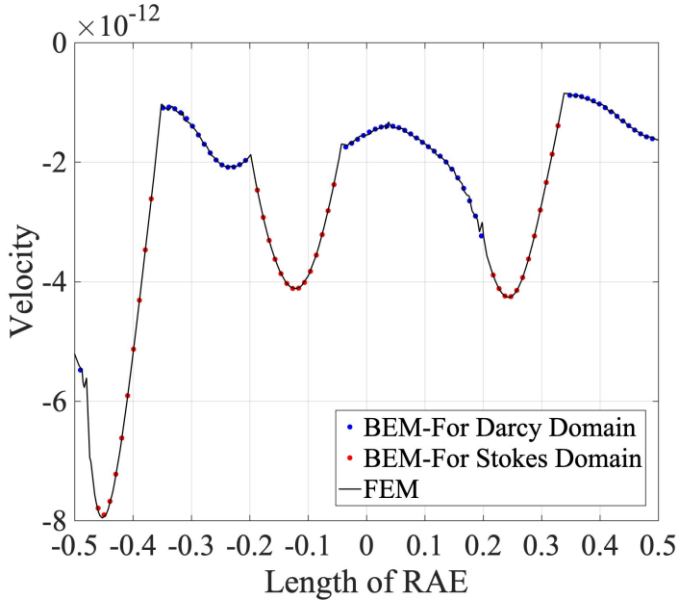

Figure 5. Variation and comparison of the normalized velocity field on the line y=-0.1.

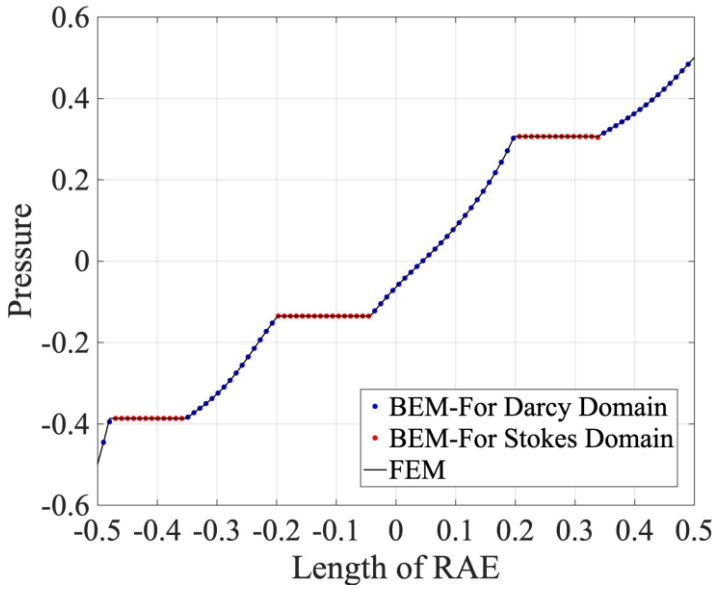

Figure 6. Variation and comparison of the normalized pressure field on the line y=-0.1.

The second example is related to a porous material consisting of a host solid matrix in which elliptical fluid-filled inclusions of arbitrary sizes are inserted. Using the Eq. (11) together with Eqs. (13) and (14), we show in Fig. 7 the corresponding estimate for the normalized effective permeability k^{eff} versus area fraction ϕ of inclusions. It can be seen from Fig. 7 that the effective permeability augments with the increase of the area fraction.

Finally, to illustrate the influence of the slip coefficient, the geometrical properties and the area fraction of pore inclusion on the effective permeability, we consider, in the third example, doubly porous materials consisting of a solid matrix phase containing identical fluid-filled inclusions whose the shape is elliptical. In this example, three cases with the slip coefficient $\lambda = 0$, $\lambda = 2$ and $\lambda = 5$ are studied. For each case, the area fraction of fluid-filled inclusions is set to vary with $\phi = 0.05, 0.1, 0.15, 0.2$ and the aspect ratio $w = a/b$ of the

elliptical pore varies from 0.2 to 1. Note that, the normalized permeability of the host solid matrix is allways kept constant with $k = 0.01$.

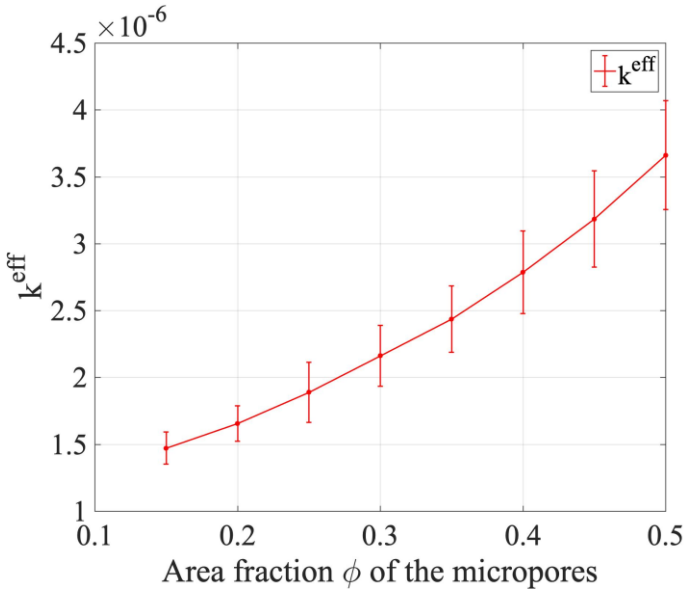

Figure 7. Normalized effective permeability versus the area fraction of fluid-filled inclusions.

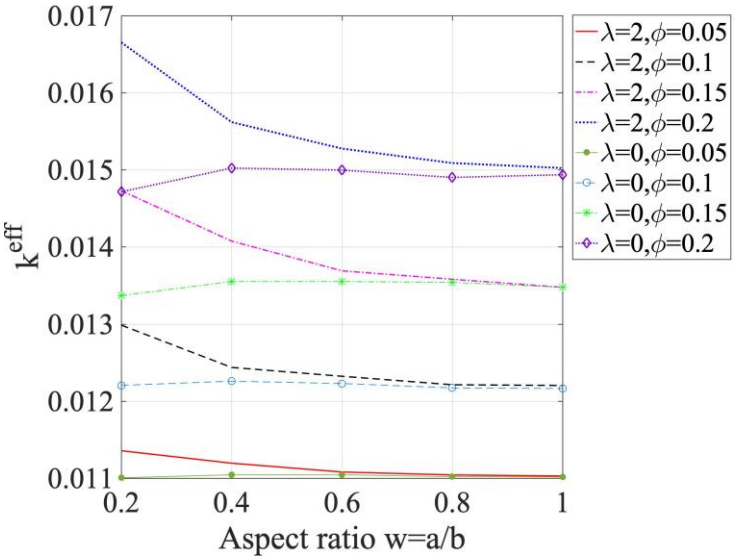

Figure 8. Normalized effective permeability versus the aspect ratio of fluid-filled inclusions.

We plot in Figs. 8 and 9 the variation of the normalized effective permeability of porous material under investigation in terms of aspect ratio of the elliptical pore for all cases mentioned above. It can be seen from Fig. 8 and 9 that: (*i*) The macroscopic permeability k^{eff} augments with the increase of the porosity ϕ; (*ii*) For a given values of the porosity ϕ and slip coefficient λ, the effective permeability k^{eff} increases when the aspect ratio w decreases (the pore becomes more elongated); (*iii*) When the value of interfacial parameter λ reduces, respectively, the effective permeability k^{eff} reduces.

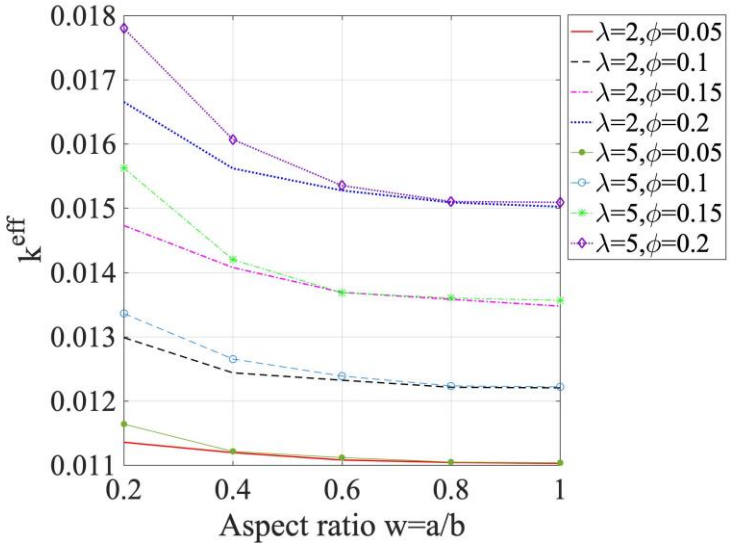

Figure 9. Normalized effective permeability versus the aspect ratio of fluid-filled inclusions.

4. CONCLUSION

In recent years, investigations on doubly porous materials have been captured the attention of a good number of researchers. In the present research work, the estimation of the macroscopic permeability of doubly porous materials consisting of a solid matrix phase with fluid-filled inclusions has been obtained by applying the Boundary Element Method (BEM). In order to understand the role of the interfacial parameter, the geometrical properties of pores and the porosity on the effective permeability of double porosity materials, some numerical examples have been considered. The results obtained from the our elaborated approach have been compared with the numerical ones provided by the Finite Element Method. This comparison has confirmed the accuracy and efficiency of our method and all the results presented in this work. Finally, due to the mathematic analogy existing between different transport phenomena, all results obtained in the present work for effective permeability of doubly porous materials can be straightforwardly transposable to any other transport problems such as electric conduction, thermal conduction, dielectrics, magnetism, diffusion as well as acoustic problem.

ACKNOWLEDGMENT

This research is funded by University of Transport and Communications (UTC) under grant number T2023-CT-003TĐ.

REFERENCES

[1]. G. S. Beavers, D. D. Joseph, Boundary conditions at a naturally permeable wall, J.Fluid. Mech., 30 (1967) 197–207. https://doi.org/10.1017/S0022112067001375

[2]. P. G. Saffman, On the boundary condition at the surface of a porous medium, Stud. Appl. Math., L2, (1971) 93-101. https://doi.org/10.1002/sapm197150293

[3]. J. L. Auriault, E. Sanchez-Palencia, Etude du comportement macroscopique d'un milieu poreux saturé déformable, J. Mecanique, 16 (1977) 575-603.

[4]. E. Sanchez-Palencia, Non-homogeneous media and vibration theory, Lecture Notes in Physics, 127 (1981). https://doi.org/10.1007/3-540-10000-8

[5]. S. Whittaker, Diffusion and dispersion in porous media, AlchE J., 13 (1967) 420-432. https://doi.org/10.1002/aic.690130308

[6]. J. Barrere, J. -P. Caltagirone, O. Gipouloux, Détermination numérique de la perméabilité en mileu poreux périodique tridimensionnel, C. R. Acad. Sci., 310 (1990) 347-352.

[7]. D. Cioranescu, P. Donato, H. I. Ene, Homogenization of the Stokes problem with non-homogeneous slip boundary conditions, Math. Methods Appl. Sci., 19 (1996) 857-881. https://doi.org/10.1002/(SICI)1099-1476(19960725)19:11<857::AID-MMA798>3.0.CO;2-D

[8]. F. Alcocer, P. Singh, Permeability of periodic porous media, Phys. Rev. E, 59 (1999) 771. https://doi.org/10.1103/PhysRevE.59.711

[9]. F. Alcocer, P. Singh, Permeability of periodic arrays of cylinders for viscoelastic flows, Phys. Fluids, 14 (2002) 2578-2581. https://doi.org/10.1063/1.1483301

[10]. H. -B. Ly, B. Le Droumaguet, V. Monchiet, D. Grande, Designing and modeling double porous polymeric materials, Eur. Phys. J. Special Topics, 224 (2015) 1689-1706. https://doi.org/10.1140/epjst/e2015-02491-x

[11]. V. Monchiet, G. Bonnet, G. Lauriat, A fft-based method to compute the permeability induced by a stokes slip flow through a porous medium, C. R. Mécanique, 337 (2009) 192-197. https://doi.org/10.1016/j.crme.2009.04.003

[12]. T. -K. Nguyen, V. Monchiet, G. Bonnet, A Fourier based numerical method for computing the dynamic permeability of periodic porous media, Eur. J. Mech. B-Fluid, 37 (2013) 90-98. https://doi.org/10.1016/j.euromechflu.2012.07.004

[13]. H. -B. Ly, V. Monchiet, D. Grande, Computation of permeability with fast Fourier transform from 3-D digital images of porous microstructures, Int. J. Numer. Methods Heat Fluid Flow, 26 (2016) 1328-1345. https://doi.org/10.1108/HFF-12-2014-0369

[14]. C. Pozrikidis, Boundary integral and singularity methods for linearized viscous flow, Cambridge University Press, Cambridge, 1992.

[15]. J. T. Katsikadelis, Boundary elements: Theory and applications, Elsevier, Amsterdam, 2002.